The EMBO Journal (2010) 29, 315–326 | © 2010 European Molecular Biology Organization | All Rights Reserved 0261-4189/10
www.embojournal.org

THE EMBO JOURNAL

Bacterial motility complexes require the actin-like protein, MreB and the Ras homologue, MglA

Emilia MF Mauriello[1,3], Fabrice Mouhamar[2,3], Beiyan Nan[1], Adrien Ducret[2], David Dai[1], David R Zusman[1,*] and Tâm Mignot[2,*]

[1]Department of Molecular and Cell Biology, University of California, Berkeley, CA, USA and [2]Laboratoire de Chimie Bactérienne CNRS UPR9043, Institut de Microbiologie de la Méditerrannée, Université Aix-Marseille, Marseille, France

Gliding motility in the bacterium *Myxococcus xanthus* uses two motility engines: S-motility powered by type-IV pili and A-motility powered by uncharacterized motor proteins and focal adhesion complexes. In this paper, we identified MreB, an actin-like protein, and MglA, a small GTPase of the Ras superfamily, as essential for both motility systems. A22, an inhibitor of MreB cytoskeleton assembly, reversibly inhibited S- and A-motility, causing rapid dispersal of S- and A-motility protein clusters, FrzS and AglZ. This suggests that the MreB cytoskeleton is involved in directing the positioning of these proteins. We also found that a Δ*mglA* motility mutant showed defective localization of AglZ and FrzS clusters. Interestingly, MglA–YFP localization mimicked both FrzS and AglZ patterns and was perturbed by A22 treatment, consistent with results indicating that both MglA and MreB bind to motility complexes. We propose that MglA and the MreB cytoskeleton act together in a pathway to localize motility proteins such as AglZ and FrzS to assemble the A-motility machineries. Interestingly, *M. xanthus* motility systems, like eukaryotic systems, use an actin-like protein and a small GTPase spatial regulator.

The EMBO Journal (2010) **29,** 315–326. doi:10.1038/emboj.2009.356; Published online 3 December 2009
Subject Categories: cell & tissue architecture; microbiology & pathogens
Keywords: A22; adhesion complexes; cell polarity; motility clusters; protein localization

*Corresponding authors. DR Zusman, Department of Molecular and Cell Biology, University of California, 16 Barker Hall, Berkeley, CA 94720-3204, USA. Tel.: +1 510 642 2293; Fax: +1 510 642 7038; E-mail: zusman@berkeley.edu or
T Mignot, Laboratoire de Chimie Bactérienne, Institut de Microbiologie de la Méditerrannée, 31 Chemin Joseph Aiguier, Marseille 13009, France. Tel.: +33 491164513; Fax: +33 491718914; E-mail: tmignot@ifr88.cnrs-mrs.fr
[3]These authors contributed equally to this work
We would like to dedicate this paper to the memory of Jean Marc Reyrat, friend and colleague.

Received: 19 March 2009; accepted: 28 October 2009; published online: 3 December 2009

Introduction

Bacterial motility is important for a wide variety of biological functions such as swarming, chemotaxis, biofilm formation, and virulence. For example, the Gram-negative bacterium *Myxococcus xanthus* exhibits a complex life cycle that includes swarming, predation, and fruiting body formation: motility is important for all of these functions. *M. xanthus* does not contain flagella, but is able to move across solid surfaces using two very different motility systems (Hodgkin and Kaiser, 1979). The first motility system, called social (S-) motility, is similar to twitching motility in *Pseudomonas aeruginosa* and is powered by type-IV pili localized at the leading cell pole (Wall and Kaiser, 1999). Cell movement occurs because the polar pili bind to polysaccharides on the substrate or on the surface of other cells: this triggers pilus retraction, which pulls the cells forward (Wall and Kaiser, 1999; Sun *et al*, 2000; Li *et al*, 2003). The second motility system, called adventurous (A-) motility, is still not very well understood. Multiple genetic screens have led to the identification of over 40 genes required for A-motility, but their specific functions are mostly uncharacterized and a molecular motility engine has not been identified (Rodriguez and Spormann, 1999; Youderian *et al*, 2003; Yu and Kaiser, 2007). During the last 40 years, many models have been proposed to explain the mechanism of A-motility, including surfactant effects, moving chains of adhesions, rotating membrane embedded rotors, and, more recently, slime extrusion through nozzles (Wolgemuth *et al*, 2002; Mignot, 2007). However, clear-cut evidence for any of these models has been lacking.

Recently, several findings suggested that A-motility involves distributed motors and focal adhesion complexes. For example, observations of filamentous cells indicated that the A-motility gliding motors are not located at the lagging cell pole, but distributed along the cell bodies (Sun *et al*, 1999; Sliusarenko *et al*, 2007). Furthermore, cytological studies showed that AglZ, an A-motility protein (Yang *et al*, 2004), is localized in clusters that originate at the leading cell pole. As cells moved forward, the clusters were localized at regular intervals along the cell body, where they remained at fixed positions relative to the substratum (Mignot *et al*, 2007). Based on this evidence, it was proposed that the AglZ clusters were associated with A-motility motors that power motility by coupling movement on a rigid cytoskeletal filament with adhesion complexes on the surface (Wozniak *et al*, 2004; Mignot, 2007; Mignot *et al*, 2007). This proposed motility mechanism has similarities to eukaryotic focal adhesion complexes, where cell-surface ligands that provide anchor points with the extracellular matrix are connected to the actin–myosin network in the interior of the cell (Wozniak *et al*, 2004).

Motility in *M. xanthus* exhibits an additional complexity in that cells periodically reverse. During reversals, which usually occur about every 7–14 min depending on the cultural

conditions, the polarity of cells inverts. Thus, the leading cell pole becomes the lagging pole and the old lagging pole becomes the new leading pole (Mauriello and Zusman, 2007). During cell reversals, the A- and S-engines reverse direction coordinately. For example, the S-motility protein FrzS and the A-motility protein AglZ are transferred together from the old to the new leading pole (Ward *et al*, 2000; Yang *et al*, 2004; Mignot *et al*, 2005, 2007). At the same time, proteins associated with the lagging cell pole, like the A-motility protein RomR (Leonardy *et al*, 2007), track to the new lagging pole. The frequency of cell reversals is controlled by the Frz (*frizzy*) signal transduction system (Blackhart and Zusman, 1985). It is hypothesized that periodic cell reversals allows cells to reorient themselves to achieve directed motility (Zusman *et al*, 2007). Thus, most *frz* mutants rarely reverse and are defective in swarming and fruiting body formation; in contrast, some *frz* mutants hyper-reverse and form very compact colonies as the cells show very little net surface translocation (Bustamante *et al*, 2004).

In this paper, we identified the actin-like protein MreB and the Ras-like protein MglA as critical components in the localization of the A- and S-motility proteins, FrzS and AglZ. We also found that MreB acts upstream of MglA in the positioning of polar motility proteins and the focal adhesion complexes. Finally, our data suggest that assembly of the focal adhesion clusters is an essential requirement for cells to achieve A-motility.

Results

MreB forms helical cytoskeletal filaments in M. xanthus cells

MreB is an actin-like protein found in rod-shaped bacteria (Jones *et al*, 2001; Kruse *et al*, 2003; Gitai *et al*, 2005). It shares structural similarities with the eukaryotic actin, but differs in its amino-acid sequence. It has been shown that MreB is a major bacterial cytoskeletal protein, forming a helical scaffold that spans the length of the cells (Jones *et al*, 2001; Kruse *et al*, 2003; Gitai *et al*, 2005). MreB is an essential protein required for correct assembly of new peptidoglycan (Gitai *et al*, 2004; Leaver and Errington, 2005; Divakaruni *et al*, 2007; Mohammadi *et al*, 2007); indeed, depletion of MreB from *Escherichia coli*, *Bacillus subtilis*, or *Caulobacter crescentus* causes cells to round up and lyse (Varley and Stewart, 1992; Jones *et al*, 2001; Kruse *et al*, 2003; Figge *et al*, 2004; Gitai *et al*, 2004; Slovak *et al*, 2005). We hypothesized that MreB may play a role in A-motility, perhaps by positioning focal adhesion sites, since previous results from our laboratory showed that the A-motility protein, AglZ, is associated with clusters that are distributed along the length of cells, displaying a periodicity that matches the helical pitch of MreB from other bacteria (Kruse *et al*, 2003; Defeu Soufo and Graumann, 2005; Mignot *et al*, 2007). To test this hypothesis, we decided to characterize the *M. xanthus* MreB protein at the cellular level.

The *mreB* gene was identified in the annotated *M. xanthus* genome as a single gene transcriptional unit (Arshinoff *et al*, 2007) (http://xanthus.wikimods.org/cgi-bin/gene_page.pl?feature_id=973046); it is not part of an operon with *mreC* and *mreD* as in *B. subtilis* and *E. coli* (Varley and Stewart, 1992; Kruse *et al*, 2003). We cloned and expressed a His-tagged fragment (202 C-terminal residues) of *M. xanthus* MreB in *E. coli*, purified the protein, and prepared rabbit anti-MreB antibodies (Supplementary Figure S1). Purified anti-MreB antibodies were then used to determine the localization of MreB in wild-type *M. xanthus* cells by deconvolution microscopy using fixed, permeabilized, and stained cells. The micrographs shown in Figure 1A show that MreB from *M. xanthus* is similar to MreB seen in other bacterial species, appearing to form helical filaments that span the length of the cells. Additionally, the apparent pitch of the helices (0.47 ± 0.1 μm, average of six cells) was also similar to those observed in *E.coli* and *B. subtilis* (Kruse *et al*, 2003; Defeu Soufo and Graumann, 2005). These results show that *M. xanthus* indeed assembles a MreB cytoskeleton and that this cytoskeleton shows a periodicity that matches the

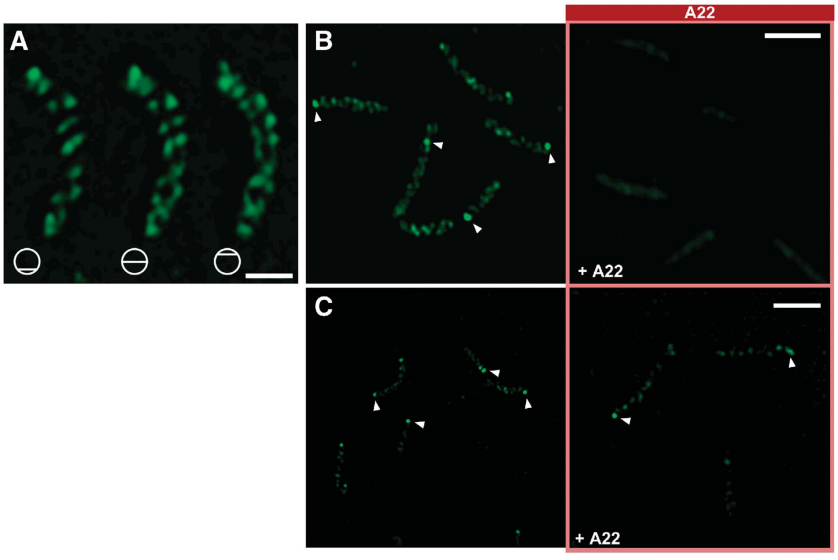

Figure 1 MreB forms an A22-sensitive helix in *M. xanthus*. (**A**) Shown are deconvolved *z* stacks (bottom, middle, and top) of a single wild-type cell stained with anti-MreB purified antibodies. Scale bar = 1 μm. (**B**) Immunofluorescence micrographs of wild-type cells treated or not (right and left panel, respectively) with A22 (150 μg/ml). Arrows point to MreB-enriched clusters at the cell poles. Scale bar = 2 μm. (**C**) Same experiment as in panel **B**, with $mreB_{V323A}$ cells.

proposed A-motility adhesion sites (based on observed AglZ–YFP clusters) described previously (Mignot *et al*, 2007). Interestingly, brighter foci of MreB-specific fluorescence intensity were frequently observed at one cell pole, suggesting the existence of a pole-specific cytoskeletal structure (Figure 1B).

A22 inhibits the assembly of MreB cytoskeletal filaments in M. xanthus

To explore the hypothesis that the MreB cytoskeleton was important for A-motility, we wanted to determine whether disrupting this cytoskeleton might block A-motility. Unfortunately, we were unsuccessful at isolating an *mreB*-null mutant, suggesting that MreB may be essential in *M. xanthus* as in many other bacteria (Varley and Stewart, 1992; Jones *et al*, 2001; Kruse *et al*, 2003; Figge *et al*, 2004; Slovak *et al*, 2005). An alternative approach was to try to inhibit MreB filament assembly. A22 is a small molecule that has been shown to rapidly and reversibly depolymerize the MreB cytoskeleton and induce spherical cells in rod-shaped, Gram-negative bacteria (Iwai *et al*, 2002; Gitai *et al*, 2005). Addition of A22 to liquid cultures of exponentially growing *M. xanthus* cells resulted in the depolymerization of the MreB helices (Figure 1B, right panel). To further test the effect of A22 on MreB, cell shape perturbations were monitored after spotting *M. xanthus* cells on agar containing A22 (50 μg/ml). As control, *E. coli* cells expressing mCherry were also spotted on the agar pads at a 1:10 ratio with *M. xanthus* cells. A22 induced the formation of spherical cells in both species with comparable kinetics (Supplementary Figure S2A).

To ensure that MreB was the direct target of A22, we constructed a mutant that produced MreB with a valine-to-alanine substitution at position 323 (V323A), since this mutation in other bacterial species has been reported to significantly reduce the binding of A22 to MreB, with only moderate reductions in MreB function (Gitai *et al*, 2005; Bean *et al*, 2009). This altered *mreB* gene was then introduced into *M. xanthus* where it replaced the wild-type copy of the gene. *M. xanthus* $mreB_{V323A}$ showed wild-type growth rates in the absence of A22 (data not shown). Immunofluorescence staining revealed that $MreB_{V323A}$ localization in *M. xanthus* cells was indistinguishable from that of MreB, even when the cells were treated with A22 concentrations as high as 150 μg/ml; this indicates that A22 probably does not bind to $MreB_{V323A}$ at the concentrations tested (Figure 1C).

Perturbation of the MreB cytoskeleton blocks M. xanthus motility

To determine the importance of the MreB cytoskeleton in *M. xanthus* motility, we used a recently developed flow chamber system to follow cellular movements and fluorescently tagged motility proteins while exposed to the MreB inhibitor, A22 (see section Materials and methods; Ducret *et al*, 2009). To test the chamber, we exposed *E. coli* cells expressing a functional MreB–$mCherry_{sw}$ fusion (Bendezú *et al*, 2009) to A22 (150 μg/ml). As expected, A22 caused rapid depolymerization of MreB–$mCherry_{sw}$; however, when A22 was removed by washing, reconstitution of MreB filaments was observed (Supplementary Figure S2B). This experiment shows that the effects of A22 are reversible in *E. coli* as they are in *C. crescentus* (Gitai *et al*, 2005), and that reversibility can be reproduced in our flow chamber. However, we note that, in this assay, while most of the cells showed reconstitution of MreB filaments, some of the cells failed to recover and instead showed aggregated MreB–$mCherry_{sw}$ (Supplementary Figure S2B).

Figure 2A and B show that exposure of isolated wild-type *M. xanthus* cells to A22 (50 μg/ml) led to complete arrest of motility within 5 min in 100% of the cells ($n = 50$), indicating requirement of an assembled MreB cytoskeleton for *Myxococcus* motility. To strengthen the correlation between the observed arrest of motility and the perturbation of the MreB cytoskeleton, we also tested whether the effect of A22 on cell movement was reversible. Significantly, motility recovered in 75% of the cells 6–7 min after removing A22 (Figure 2B and Supplementary data for statistical analysis of the data). The fact that the whole cell population did not recover may be explained by MreB aggregation in some cells after removal of A22, as observed in *E. coli* (Supplementary Figure S2B). This could not be verified in the absence of a functional *Myxococcus* MreB fluorescent fusion. However, as control we also tested the effect of A22 (50 μg/ml) on the motility of *M. xanthus* $mreB_{V323A}$ cells. We found that A22 injections did not affect the motility of $mreB_{V323A}$ cells significantly, indicating that the effect of A22 on motility is MreB-dependent and not due to the experimental condition used in the assay (Figure 2A and C).

Perturbations of the cytoskeleton block both A- and S-motility

To determine how A22 affects the two different motility systems of *M. xanthus*, we placed cells exhibiting only A-motility (A^+S^-) or S-motility (A^-S^+) in the flow chamber. For this experiment, A-motile and S-motile cells were mixed to monitor the effect of A22 on each motility system simultaneously as A22 was injected (150 μg/ml; see section Materials and methods). Figure 3A shows that injection of A22 led to complete arrest of isolated A^+S^- cells, suggesting requirement of an assembled MreB cytoskeleton for A-motility. To study S-motility in A^-S^+ cells, we tracked cells in groups, as isolated S-motile cells are non-motile (Hodgkin and Kaiser, 1979). A22 also blocked motility in the A^-S^+ cells, with kinetics similar to those seen for A-motility (Figure 3A). To strengthen the correlation between the observed arrest of motility and the perturbation of the MreB cytoskeleton, we also tested whether the effect of A22 on cell movements was reversible. Figure 3A shows that both A- and S-motility resumed 10 min after removing A22.

A22 disrupts the localization of AglZ motility clusters

As described previously, AglZ is an A-motility protein playing a regulatory function and is associated with distributed clusters that show periodicity similar to that of MreB (Mignot *et al*, 2007; Mauriello *et al*, 2009). If MreB acts as a cytoplasmic anchor for these clusters, we would predict that disruption of the MreB cytoskeleton with A22 would cause these clusters to disperse. In order to test this hypothesis, we followed the localization of AglZ–YFP in our flow chamber system by analysing the kinetics of AglZ–YFP cluster dispersal upon injection of A22 (50 μg/ml) and checking whether the effects were reversible. Figure 3B shows a fluorescence microscopy time-lapse sequence of AglZ–YFP clusters after addition and removal of A22. We found that the disappearance

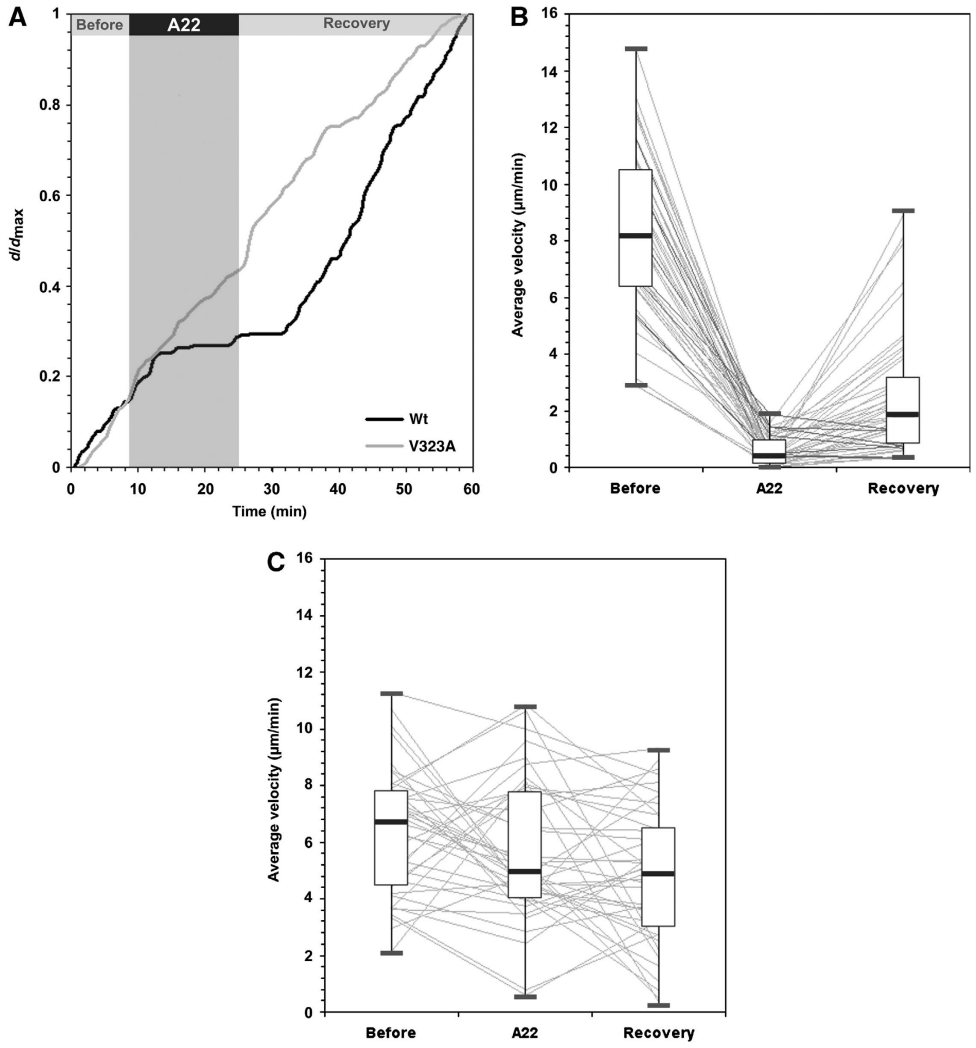

Figure 2 (**A**) Effect of A22 on the motility of wild-type cell. The relative cumulative distance corresponding to the distance travelled by wild-type (black line) or $mreB_{V323A}$ (grey line) cells at a given time over the maximum travelled distance of that same cell at the end of the time lapse (d/d_{max}) are plotted over time. The grey rectangle indicates the time interval when the cells were in the presence of A22 (50 μg/ml). (**B**) Box plots of wild-type cell ($n = 50$) velocities before, during, and after treatment by A22. The solid black bars represent the average velocity of the population during each condition. Each line represents a single cell before, during, and after treatment. Darker lines represent cells showing no obvious recovery. (**C**) Box plots of $mreB_{V323A}$ cells ($n = 50$). Legend reads as in panel **B**.

and re-appearance of AglZ–YFP clusters followed the same time course as loss and restoration of A-motility (Figure 3A and B).

To investigate whether MreB and AglZ interact as part of a complex, we performed *in vitro* cross-linking experiments using isolated AglZ polypeptides, since the intact protein was very large (1395 amino acids) and therefore difficult to analyse. In these experiments, the N-terminal pseudo-receiver domain of AglZ ($AglZ^{Rec}$, residues 2–240) and a fragment corresponding to the tandem coiled-coil domain of AglZ ($AglZ^{coil}$, residues 230–1384) (Mauriello *et al*, 2009) were purified (Figure 4B) and mixed with purified full-length MreB in the presence of the cross-linking agent, formaldehyde. The interaction products were analysed by western immunoblotting, using purified anti-AglZ antibodies (Figure 4C). The appearance of new higher molecular weight bands in samples containing the coiled-coil domain of AglZ but not the N-terminal domain of AglZ showed that MreB specifically interacts with that domain. Interestingly, this interaction could be increased by addition of ATP to the incubation mixture, suggesting that AglZ binds preferentially when MreB is in its polymerized state (Figure 4C).

A22 disrupts the localization of the S-motility protein, FrzS

FrzS is an S-motility protein that shows bipolar localization, with most FrzS found at the leading cell pole, the pole that contains the pili that power S-motility (Sun *et al*, 2000). Since A22 also inhibits S-motility (Figure 3A), we were interested in determining whether A22 affects the localization of FrzS. When we treated FrzS–GFP-expressing *M. xanthus* cells (Mignot *et al*, 2005) with A22 (50 μg/ml) in our flow chamber apparatus, complete and reversible dispersal of FrzS localization was observed upon addition and subsequent removal of A22 (Figure 3C). The dispersal and reconstitution of the polar FrzS clusters also followed the same time course as loss and restoration of S-motility (Figure 3A and C). We were unable to detect an interaction between MreB and FrzS by *in vitro*

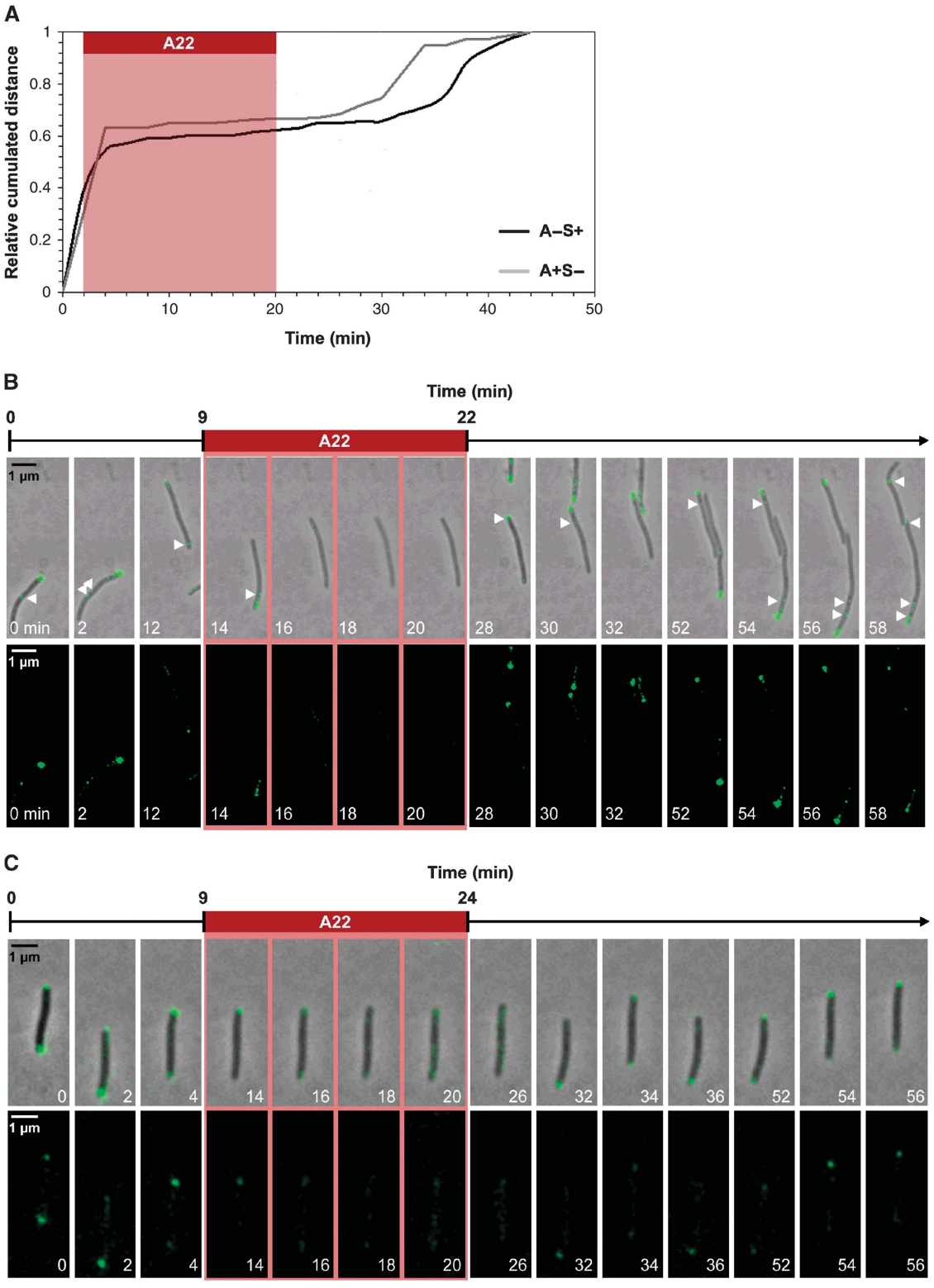

Figure 3 MreB is required for both A- and S-motility. (**A**) Effect of A22 (150 μg/ml) on the motility of A^+S^- (grey line) and A^-S^+ cells (black line). (**B**) Effect of A22 (50 μg/ml) on the localization of AglZ–YFP. Phase-contrast (grey) and corresponding fluorescence micrographs (green) were overlaid and shown at different time points (top panel). The original fluorescence micrographs are also shown (bottom panel). White arrows point to internal fixed clusters observable before and after A22 treatment. (**C**) Effect of A22 (50 μg/ml) on the localization of FrzS–GFP.

cross-linking, suggesting that the proteins do not interact directly or that the conditions for interaction were not reconstituted in the assay (data not shown).

The kinetics of A22 motility inhibition and recovery are similar for both A- and S-motility systems, as reflected by the corresponding perturbations of FrzS–GFP and AglZ–YFP localizations. To test whether A22 perturbations for these motility systems are indeed synchronized, we constructed a strain that coexpressed AglZ–mCherry (Mauriello *et al*, 2009) and FrzS–GFP (Mignot *et al*, 2005). As expected, we found

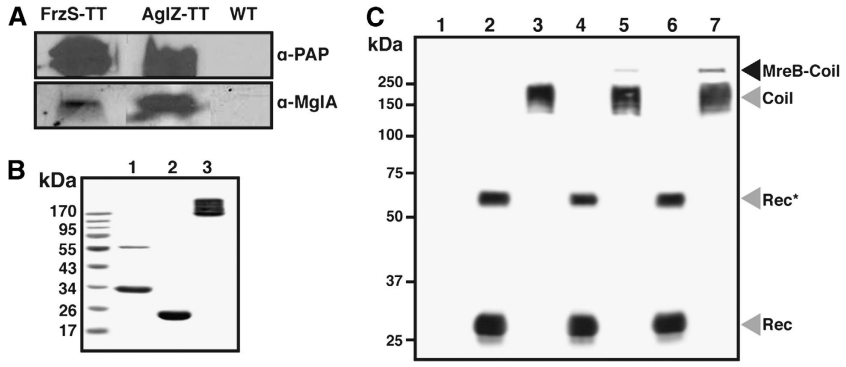

Figure 4 Protein interactions between MreB, MglA, FrzS, and AglZ. (**A**) MglA interacts with FrzS and AglZ. Western blots of calmodulin bead eluates to detect the co-presence of either FrzS–TT and MglA or AglZ–TT and MglA using anti-PAP and anti-MglA antibodies. Eluates from the extracts of wild-type cells that do not express the Tap-tagged variants are run as controls. (**B**) Coomassie-stained SDS–polyacrylamide gel of recombinant MreB (lane 1), $AglZ^{Rec}$ (lane 2), and $AglZ^{coil}$ (lane 3). The presence of multiple bands in the purified samples of $AglZ^{coil}$ (lane 3) may reflect multiple oligomerization states, which has been previously described (Mauriello *et al*, 2009). (**C**) Anti-AglZ western immunoblot of reaction samples containing purified MreB and/or AglZ domains after incubation in formaldehyde (10 mM) and ATP (2 mM) (ATP was only added in lanes 1–3, 6, and 7). Lanes 1–3: MreB, $AglZ^{Rec}$, or $AglZ^{C\text{-}coil}$ incubated alone; lanes 4 and 5: MreB co-incubated with $AglZ^{Rec}$ or $AglZ^{C\text{-}coil}$; lanes 6 and 7: MreB co-incubated with $AglZ^{Rec}$ or $AglZ^{C\text{-}coil}$ in the presence of ATP. The black arrow indicates a high-molecular-weight band that only becomes visible when MreB is mixed with $AglZ^{coil}$. Rec*, pseudo-receiver domain dimer.

that A22 treatment and removal affected AglZ–mCherry and FrzS–GFP dynamics coordinately, suggesting a direct co-dependence of both A- and S-motility upon intact MreB cytoskeleton (Supplementary Figure S3).

MglA is also required for the localization of motility proteins

mglA was identified by Hodgkin and Kaiser (1979) as the only gene whose function was required for both A- and S-motility. The Hartzell laboratory showed that MglA interacts directly with AglZ (Yang *et al*, 2004). Moreover, bioinformatic and genetic analyses indicate that MglA is a monomeric GTPase of the Ras family, a class of proteins that has been studied primarily in eukaryotic cells where they perform a broad range of functions, including transport, signal transduction, and cell migration (Hartzell and Kaiser, 1991a; Hartzell, 1997; Charest and Firtel, 2007). In order to study the role of MglA in *M. xanthus* motility, we constructed an *mglA* in-frame deletion mutant (Supplementary Figure S4), as some of the previously described *mglA* mutants showed differing phenotypes. For example, it was reported that a missense mutation in *mglA* was completely non-motile (Stephens, 1987; Hartzell and Kaiser, 1991a; Leonardy *et al*, 2007), whereas a Δ*mglBA* mutant was motile but hyper-reversing (Rodriguez and Spormann, 1999). Our *mglA* in-frame deletion mutant failed to swarm on either soft or hard agar as expected (Supplementary Figure S4B), although, in our experiments some isolated Δ*mglA* cells showed occasional sporadic twitching (data not shown).

To confirm that MglA is a bona fide Ras-like GTPase, we purified MglA to test its ability to hydrolyse GTP. Purification of recombinant MglA proved difficult as the protein aggregated very quickly during dialysis. Addition of 10 μM GDP to the dialysis buffer prevented aggregation suggesting that GDP is important for the stability and conformation of MglA (data not shown). Using an *in vitro* enzyme-coupled assay, we were able to observe low but detectable dose-dependent MglA GTPase activity with our purified enzyme, showing that MglA indeed has GTPase activity (with a maximum measured rate of 40 s^{-1}; Figure 5A).

To study the role of MglA in *M. xanthus* motility, we followed the localization of AglZ–YFP and FrzS–GFP fusions in Δ*mglA* cells. In Δ*mglA* cells expressing AglZ–YFP, AglZ failed to localize as multiple clusters along the cell length like the wild type, and only a minority of cells contained a faint transient cluster at one cell pole (Figure 5B). In Δ*mglA* cells expressing FrzS–GFP, FrzS localized at only one cell pole, rather than both cell poles, which is typical for the wild-type strain (Figure 5C). The localization of AglZ–YFP and FrzS–GFP in Δ*mglA* mutants was not the result of protein instability, as AglZ–YFP and FrzS–GFP were stably expressed in all strains (Supplementary Figure S5).

MglA was previously shown to interact with AglZ by yeast two-hybrid analysis (Yang *et al*, 2004). To confirm this interaction in *M. xanthus* and determine whether MglA also interacts with FrzS, we constructed strains that expressed AglZ or FrzS fused to tandem affinity purification (TAP) tags (Puig *et al*, 2001) (AglZ–TT and FrzS–TT) from the endogenous loci. These strains showed no detectable defects in A- or S-motility (data not shown). Cell lysates from each strain were subsequently analysed as described under Materials and methods. Figure 4A shows that MglA was only detected in eluates containing AglZ–TT and FrzS–TT complexes, indicating that MglA interacts with both AglZ and FrzS. Taken together these results suggest that MglA acts directly on FrzS and AglZ to recruit these proteins to their sites of action.

Localization of MglA in moving cells requires the MreB cytoskeleton

To follow MglA localization in moving cells, we constructed a strain in which an *mglA*::*yfp* fusion replaced the wild-type copy of *mglA* (Supplementary Figure S4). In this strain, MglA–YFP was stably expressed and colonies clearly displayed motility, although they showed slightly reduced swarming as compared with the wild type (Supplementary Figure S6). However, since single cells moved at velocities comparable to wild-type, we considered the *mglA*::*yfp* strain a useful tool to investigate the dynamics of MglA–YFP *in vivo*. Figure 6A shows that MglA–YFP localizes at both cell poles following the pattern of FrzS, but also as clusters along the

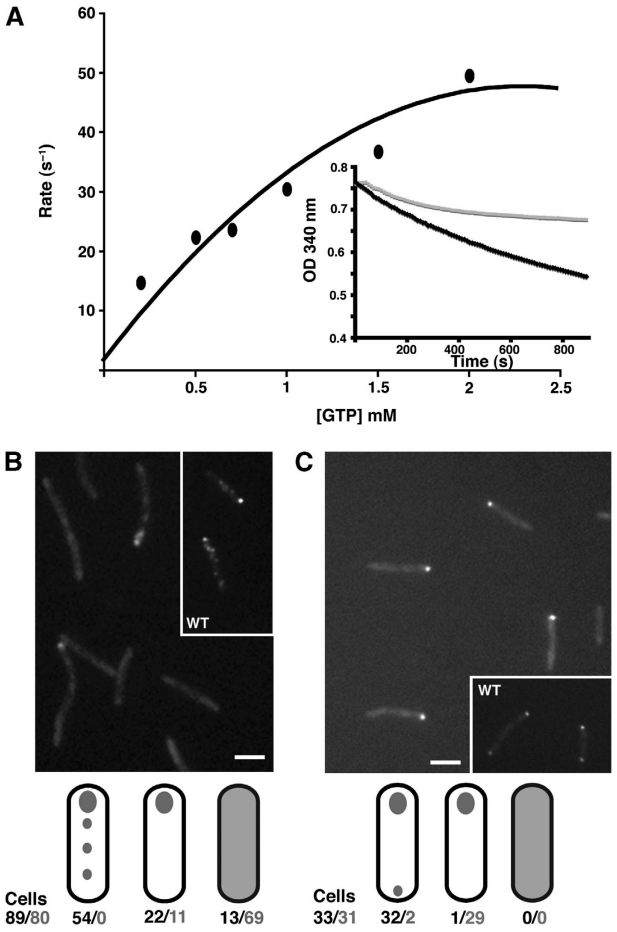

Figure 5 MglA has GTPase activity and is required for localization of motility proteins. (**A**) *In vitro* hydrolysis of GTP by recombinant MglA. The calculated reaction rates of hydrolysis (see section Materials and methods) as a function of the concentration of GTP are shown. Inset: 340-nm NADH absorbance in the presence (black line) or absence (grey line) of MglA after reaction initiation over time (s). (**B**) MglA is necessary for localization of AglZ–YFP. Micrographs showing localization of AglZ–YFP in an *mglA* strain. Inset: Localization of AglZ–YFP in a wild-type background. The cartoon represents cells with different localization patterns and their relative numbers for the wild-type strain (black) and for the *mglA* mutant (grey). Scale bar = 1 μm. (**C**) MglA is necessary for bipolar localization of FrzS–GFP. Legends read as in panel A.

cell length following the pattern of AglZ (Figure 6A and B). Thus, the MglA localization pattern mimics both FrzS and AglZ patterns. However, MglA–YFP localization was not affected by the absence of AglZ (Supplementary Figure S7) or FrzS (data not shown). These results confirm that MglA acts upstream of FrzS and AglZ in the regulation of motility.

To determine whether the MreB cytoskeleton is required for MglA localization, we placed the MglA–YFP-expressing cells in our flow chamber and exposed them to A22. Figure 6C shows that the MglA internal clusters were dispersed upon treatment with A22, coincident with the motility block. Interestingly, MglA–YFP was mostly found at one pole following A22 treatment, suggesting that an independent mechanism anchors MglA at the cell poles. These results show that proper positioning of the internal motility clusters directly depends on the MreB cytoskeleton. We note that the effect of A22 was only partially reversible for *mglA*::*yfp* cells. Indeed, A22 removal led to pole-to-pole oscillations of MglA–YFP, but motility did not resume significantly in the time frame studied (Figure 6C).

Discussion

Gliding motility is critical to the life cycle of many bacterial species that, like *M. xanthus*, live and move on solid surfaces. However, our knowledge of these motility systems is limited (Mignot, 2007). This study highlights the central role of two essential players of bacterial surface motility: MreB, the actin-like cytoskeleton found in most rod-shaped bacteria (Jones *et al*, 2001; Kruse *et al*, 2003; Gitai *et al*, 2005), and MglA, a small GTPase of the Ras superfamily, important for many regulated functions in eukaryotic cells (Hartzell and Kaiser, 1991a; Hartzell, 1997; Charest and Firtel, 2007). These findings suggest that although many aspects of the mechanism of bacterial surface motility are novel, elements of the motility engines may not be completely different from those found in eukaryotes.

The principal finding of this study is that MreB is essential for both A- and S-motility in *M. xanthus*, thereby revealing an unanticipated role for the bacterial cytoskeleton in gliding motility. We hypothesized a possible role for MreB in *M. xanthus* motility as our previous studies of the spatial organization of the A-motility protein AglZ showed that in moving cells AglZ is localized in clusters that are distributed at regular intervals along the length of cells and that these clusters showed periodicity similar to that found in the MreB cytoskeleton of several bacterial species (Kruse *et al*, 2003; Defeu Soufo and Graumann, 2005; Mignot *et al*, 2007). To explore this hypothesis, we characterized the MreB scaffold from *M. xanthus*. We prepared antibodies to *M. xanthus* MreB and used immunofluorescence microscopy to show that the MreB helix showed a pitch of 0.47 ± 0.1 μm, a close match to the previously observed periodicity of AglZ–YFP clusters (Mignot *et al*, 2007). Interestingly, MreB localization was enriched at the cell poles, although the function for this unexpected observation is unknown.

To obtain evidence that the cytoskeleton is indeed connected to the clusters, we used A22, a potent inhibitor of MreB polymerization, to reversibly inactivate the MreB cytoskeleton (Gitai *et al*, 2005). A22 is a powerful tool to study the cytoskeletal processes in bacteria as it allows one to study the effects of rapid cytoskeletal breakdown and regeneration, in contrast to MreB depletion experiments, which are much slower (Gitai *et al*, 2005). We predicted that *Myxococcus* MreB would be subject to A22 inhibition as all of the MreB A22-target residues are conserved in *M. xanthus* (Gitai *et al*, 2005). Indeed, our immunofluorescence experiments showed that A22 depolymerized MreB in *M. xanthus*. Furthermore, the behaviour of the $mreB_{V323A}$ A22-resistant mutant showed that the inhibition was specific to MreB. The inhibition of motility by A22 suggested that the MreB cytoskeleton could be involved in the positioning of many motility proteins. We therefore studied the effect of A22 on the localization of AglZ, FrzS, and MglA.

We initially speculated that MreB might recruit MglA to localize proteins such as FrzS and AglZ to their sites of action. However, our experiments suggest that the actual mechanism is probably more complex since MglA localizes to the poles and adhesion sites, but FrzS–GFP and AglZ–YFP only colocalize at the poles. We also show here that MreB

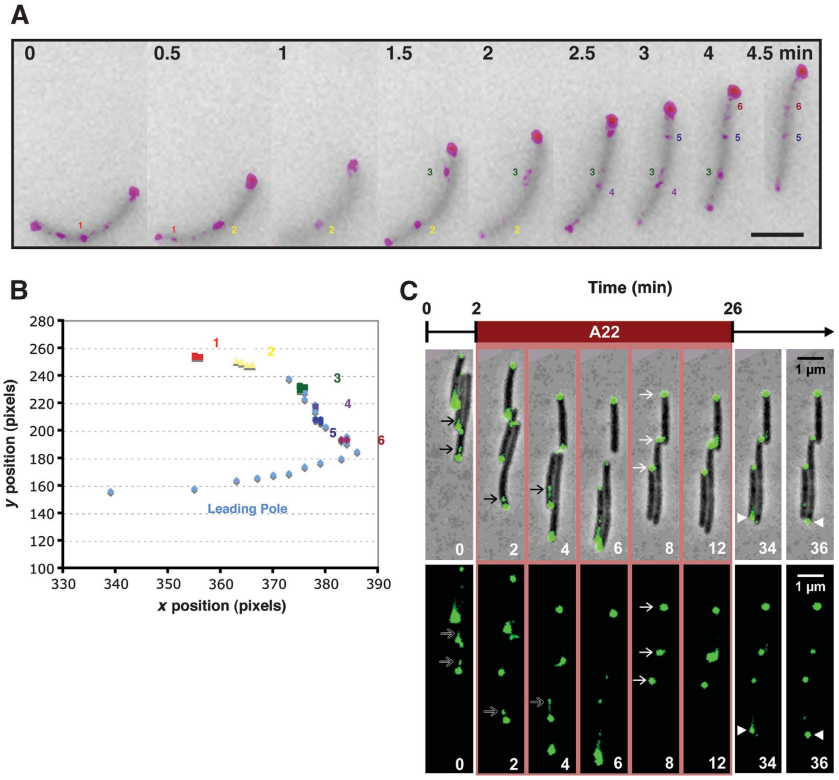

Figure 6 MglA localizes both at the poles and in clusters that remained fixed as cells move forward. (**A**) Localization of MglA–YFP in a moving cell. Phase-contrast (grey) and the corresponding fluorescent micrographs (magenta) were overlaid and artificially coloured for better clarity. The fixed clusters are numbered for the analysis shown in panel **B**. Images captured every 30 s are shown. Scale bar = 2 μm. (**B**) Internal MglA–YFP localizes within focal adhesion clusters. Positions corresponding to the leading cell pole (light blue diamonds) and the internal clusters (numbered and colour-coded in panel **A**) of the cell shown in panel **A** were tracked over time and the position coordinates of each position were plotted. (**C**) MglA–YFP localization was monitored after injection and removal of A22 (50 μg/ml). A22 causes dispersal of the internal MglA–YFP clusters (small black arrows) and results in unipolar localization (small white arrows). Images were overlaid as in Figure 3**B** and **C**. The triangles and white arrows point to pole-to-pole oscillations of MglA–YFP appearing after removal of A22. Scale bar = 1 μm.

can interact with AglZ *in vitro* in the absence of MglA. Furthermore, the localization of FrzS–GFP and AglZ–YFP in an *mglA* mutant differs from the localization pattern observed in A22-treated cells. This is especially clear in the case of FrzS, which accumulates mostly at one cell pole in the *mglA* mutant, whereas it is fully dispersed by A22 (compare Figures 3C and 5C), showing MreB-dependent but MglA-independent unipolar localization of FrzS. We therefore hypothesize that the cytoskeleton is a scaffold that acts in combination with MglA to localize motility proteins to their sites of action. This hypothesis is consistent with the following observations: (i) localization of MglA depends on MreB and, in turn, localization of S- (FrzS) and A-motility proteins (AglZ and RomR) depends on MglA (Figure 5) (Leonardy *et al*, 2007); (ii) MglA–YFP localizes at the sites of both FrzS and AglZ clusters and MglA interacts with both FrzS and AglZ (Figure 4A and Yang *et al*, 2004); and (iii) MglA is required both for cluster formation and localization as AglZ was largely mislocalized in an *mglA* mutant. Interestingly, FrzS and RomR were only found at one cell pole in the *mglA* mutant showing that MglA is specifically required for pole-to-pole trafficking of these proteins (Leonardy *et al*, 2007). Taken together these results are consistent with the hypothesis that MglA modulates motility protein localization in an MreB-dependent manner.

Sequence analysis and genetic evidence clearly indicate that MglA is a small GTPase of the Ras superfamily (Hartzell and Kaiser, 1991a; Hartzell, 1997; Charest and Firtel, 2007). Our biochemical evidence confirms that MglA is a bona fide small GTPase. *In vitro*, GTP hydrolysis occurred at relatively low rates, which is not unexpected for a small Ras-like GTPase as eukaryotic small GTPases are generally activated by GTPase-activating proteins (GAPs). In addition, the GTPase activity of MglA is most likely essential for its function as Hartzell and Kaiser (1991a) mapped loss-of-function alleles of MglA to conserved residues within the predicted catalytic site (C23F and G81V). In eukaryotic cell motility, the interplay between small GTPases and the actin cytoskeleton is well characterized: small GTPases are essential factors for focal adhesion complexes where they are recruited by actin networks, which in turn, induce network rearrangements (Wozniak *et al*, 2004). Small GTPases are also involved in regulating cell polarity during chemotaxis. In *Dictyostelium discoidum*, receptor signalling polarizes the cell, which determines directional movements. Additionally, signalling networks involving small GTPases and their cognate nucleotide exchange factors define the leading edge and the retracting edge of cells (Charest and Firtel, 2006; Kortholt and van Haastert, 2008). Our results suggest that MglA is also a polarity factor controlling the inversion of the polar localization of motility proteins during cellular reversals. Our *in vitro* experiments show that there are direct relationships between MreB, MglA, and the downstream motility proteins FrzS and AglZ; however, the precise network of protein

Table I Strains and plasmids

	Description	Source
Strain		
E. coli		
FB83	*E. coli* expressing MreB–mCherry^{sw}	Bendezú *et al* (2009)
M. Xanthus		
DZ2	Wild type	Laboratory collection
TM9	DZ2 *aglZ-yfp*	Mignot *et al* (2007)
TM12	DZ2 Δ*mglA*	This work
TM3	DZ2 *frzS-gfp*	Mignot *et al* (2005)
TM13	DZ2 *frzS-gfp mglA*	This work
TM14	DZ2 *aglZ-yfp mglA*	This work
TM17	DZ2 *mglA-yfp* (pBJmglAYR)	This work
TM27	DZ2 *mglA-yfp* Ω*aglZ* (pZeroΩ*aglZ*)	This work
TM60	DZ2 *frzS-gfp pilA*	This work
TM20	DZ2 *mglA-yfp frzS*	This work
TM263	DZ2 *aglZ-mcherry frzS-gfp*	This work
TM264	DZ2 $mreB_{V323A}$	This work
TM15	DZ2 *aglZ-taptag* (pBJAglZTT)	This work
TM31	DZ2 *frzS-taptag* (pBJFrzSTT)	This work
Plasmids		
pBJ113	Used to create deletions, *galK*, Km^R	Bustamante *et al* (2004)
pZero-2	*E. coli* Kan^R vector	Invitrogen
pZeroΩ*aglZ*	pZero-2 with a cassette allowing insertion into *aglZ*	Mignot *et al* (2007)
pJPM54	pBJ113 with a cassette allowing complete deletion of *frzS*	Mignot *et al* (2007)
pBJAglZY	pBJ113 with a cassette allowing construction of the *aglZ-yfp* chimeric gene	Mignot *et al* (2007)
pBJDmglA	pBJ113 with a deletion cassette for *mglA*	This work
pBJmglAYR	pBJ113 with a cassette allowing construction of the *mglA-yfp* chimeric gene	This work
pBJAglZTT	pBJ113 with a cassette allowing construction the *aglZ-taptag* gene	This work
pBFrzSTT	pBJ113 with a cassette allowing construction the *frzS-taptag* gene	This work

interactions will have to be defined in depth by future investigations. Other as yet unidentified factors must be involved in the complexes and dictate specificity as localization of FrzS and AglZ only overlap at the leading cell pole, whereas MglA localizes at both poles and within the adhesion clusters.

The regulation of MglA and its control over motility and protein localization may be a promising field of research: the MglA nucleotide-binding site is perfectly conserved, suggesting the existence of GDP- and GTP-bound isoforms (Supplementary Figure S8). As in *D. discoidum*, the equilibrium between the GDP- and GTP-bound states of MglA might polarize the cells and establish the *M. xanthus* cell-reversal cycle. Unfortunately, we could not determine the precise dynamics of the MglA reversal cycle because MglA–YFP is not fully functional, as this strain is slightly defective in its reversal frequency (data not shown). A search of the *Myxococcus* genome did not reveal any proteins with significant homology to known eukaryotic exchange factors. *mglB* is the gene that lies just upstream of *mglA* (Hartzell and Kaiser, 1991b). The function of MglB remains unknown, but it has been suggested that it modulates the MglA switch (Hartzell and Kaiser, 1991b; Koonin and Aravind, 2000). Clearly, more work needs to be done to investigate the connection between MglA and the cytoskeleton, as well as the role of MglB.

Previously, we hypothesized that A-motility is powered by cytoplasmic motor complexes that move on an internal cytoskeleton and couple adhesion to the substratum with motor movement (Mignot *et al*, 2007). Our findings show that that the MreB cytoskeleton is not only critical for the positioning but also for the stability of the adhesion sites. Thus, we found a central role for the cytoskeleton. However, it is not known whether the MreB cytoskeleton acts only as a passive scaffold or whether it is also the site of active traction. To answer this question, it will be necessary to identify the network of proteins that links the putative adhesion complexes and the cytoskeleton. Nevertheless, the data to date are consistent with a model in which focal adhesion clusters are required for A-motility: the arrest of A-motility is associated with AglZ cluster dispersal and, following A22 removal, recovery of motility is preceded by re-assembly of the AglZ clusters along the cell body.

In conclusion, the experiments presented show several remarkable similarities between bacterial gliding motility and eukaryotic cell migration, as both use the actin cytoskeleton and small GTPase spatial regulators. However, much additional work is needed to elucidate the details of how A-motility functions in *M. xanthus*, a bacterium that employs and coordinates two very different gliding-motility engines.

Materials and methods

Bacterial strains, plasmids, and growth

Strains and plasmids are listed in Table I. *M. xanthus* strains were grown at 32°C in casitone yeast extract (CYE)-rich media as previously described (Bustamante *et al*, 2004). Plasmids were introduced in *M. xanthus* by electroporation. Mutants and transformants were obtained by homologous recombination based on a previously reported method (Bustamante *et al*, 2004). The mode of construction of strains and plasmids, as well as the sequences of all primers, are available upon request. For the fluorescence experiments the *yfp* gene was used from the commercial vectors pEYFP-N1 (Clontech). All *M. xanthus* strains were cultured in CYE medium, which contains 10 mM MOPS (pH 7.6), 1% (w/v) Bacto Casitone (BD Biosciences), 0.5% Bacto yeast

extract, and 4 mM $MgSO_4$ (Campos *et al*, 1978). For phenotypic assays, cells (10 μl), at a concentration of 4×10^9 cfu/ml, were spotted on CF-agar plates or CYE plates containing an agar concentration of 1.5%, incubated at 32°C, and photographed after 48 h with a WTYPEI charge-coupled device (CCD)-72 camera, using a Nikon Labphot-2 or a Zeiss (model 476009-9901) microscopes.

Protein expression and purification

Proteins were expressed from the expression vector pET28(a) (Novagen). The expression was induced by growing cells at 16°C for 20 h in the presence of 0.25 mM IPTG (isopropyl-β-D-thiogalactopyranoside). Cells were then harvested by centrifugation at 8000 r.p.m. for 10 min, resuspended in a buffer containing 20 mM Tris–HCl (pH 7.4), 500 mM NaCl, 20 mM imidazol, 0.1% (w/v) CHAPS, and 10% (v/v) glycerol, and lysed by sonication on ice. The lysates were centrifuged twice (18 000 r.p.m., 4°C, 30 min) to remove debris prior to purification. Supernatants were loaded into 5 ml HisTrap nickel columns (GE Healthcare). The elution was performed by using a buffer containing 20 mM Tris–HCl (pH 7.4), 500 mM NaCl, 250 mM imidazol, 0.1% (w/v) CHAPS, and 10% (v/v) glycerol. Protein concentrations were determined by Bradford assays (Bio-Rad). For MglA purification, 10 μM GDP was added during elution and dialysis to prevent aggregation of the protein.

In vitro GTP hydrolysis assay

GTP hydrolysis was measured in a standard assay that couples hydrolysis of GTP to consumption of NADH, which is monitored by a decrease in 340-nm absorbance (Pullman *et al*, 1960). For this assay, 1 μg of MglA was resuspended at t_0 in 100 μl of reaction buffer containing MOPS–HCl (25 mM, pH 7.5), $MgCl_2$ (5 mM), EDTA (0.5 mM), NaCl (100 mM), GTP (2 mM), NADH (0.3 mM), phosphoenolpyruvate (PEP) (4 mM), pyruvate kinase (0.3 mg/ml), and lactate dehydrogenase (LDH) (0.16 mg/ml). NADH oxidation was monitored at 340 nm for 15 min. Parallel measurements in the absence of MglA were conducted to estimate spontaneous GTP hydrolysis in the reaction buffer. Also, reactions in which LDH, which drives the final step of the reaction, was omitted yielded no detectable decrease in NADH 340 nm absorbance. To measure initial the velocities of MglA-dependent hydrolysis at varying concentrations of GTP, 1 μg of MglA was incubated with GTP concentrations ranging between 0.2 and 2 mM; all reactions were stopped after 400 s. All reactions were also repeated in the absence of MglA. The reaction rates (the number of μmoles of GTP hydrolysed per μmole of MglA per second) were then calculated after subtraction of the measured spontaneous GTP hydrolysis from measured GTP hydrolysis in the presence of MglA.

Antibody purification

A 50-μg weight of recombinant MreB and AglZ fragments was run on a 1.5-mm thick, 12% SDS–PAGE gel. After electrophoresis, the gels were transferred to Trans-Blot nitrocellulose membranes (Bio-Rad). The membranes were stained with Red Ponceau and cut around the MreB and AglZ bands. These pieces of membrane were then destained with PBS–Tween and incubated in blocking solution (PBS–Tween with 5% powdered milk) overnight at 4°C. The next day, the membrane was incubated with 100 μl of anti-MreB and anti-AglZ serum, and diluted in 1 ml blocking solution for 2 h at room temperature. The membrane was then washed repeatedly with PBS–Tween and bound antibodies were eluted in 1 ml of 0.1-M glycine–HCl solution (pH 2.9) over 5 min. Neutralization prior to antibody use was obtained by adding 50 μl of 2 M Tris–HCl (pH 8) to the eluate.

Tap tag co-purification

Cultures (500 ml) of *Myxococcus* cells expressing Tap-tagged proteins were grown under constant shaking until they reached $OD_{600\,nm} = 0.5–0.6$, centrifuged, and washed three times in PBS buffer. Intracellular complexes were then cross-linked with 0.5 mM dithiobis disuccimydil proprionate (DSP; Sigma) in PBS at room temperature for 20 min. Tris–HCl (20 mM, pH 7.4) was then added to stop the reaction. The cells were centrifuged and resuspended in IPP150-calmodulin binding buffer (CBB) (10 mM Tris–HCl (pH 8.0), 150 mM NaCl, 1 mM $MgCl_2$, 1 mM imidazole, 2 mM $CaCl_2$, 0.2% Triton X-100) and broken with a French pressure cell press. Lysates were then separated from cell debris by 30-min centrifugation at 14 000 r.p.m. Lysates were then mixed with IPP150-CBB-equilibrated beads (Roche) and left to incubate for 1 h at 4°C. The beads were then collected by slow-speed centrifugation and washed four times with 1 ml of IPP150-CBB before they were eluted with IPP150-calmodulin elution buffer (IPP150-CBB, 2 mM EGTA, 10 mM β-mercaptoethanol). The eluates were then loaded on SDS–PAGE gel and probed with anti-PAP (Sigma) to detect Tap-tagged protein and anti-MglA antibodies to detect MglA.

In vitro protein cross-linking

In vitro protein cross-linking reactions were performed in 20 mM HEPES buffer (pH 8.0) 100 mM NaCl, 0.5 mM EDTA, 8% (v/v) glycerol in 20 μl final volume. Proteins were diluted to the following concentrations to keep them at a 1:1 molar ratio: MreB, 3 μg/ml; $AglZ^{Rec}$, 2 μg/ml; and $AglZ^{Coil}$, 5 μg/ml. Formaldehyde (10 mM) was then added into each pre-mixed reaction. ATP was added at a concentration of 2 mM. Reactions were stopped by adding 50 mM Tris–HCl (pH 8.0) after 20 min of incubation at room temperature. Samples (1 μl) of each reaction were used for western immunoblots.

Immunofluorescence deconvolution microscopy

Samples from vegetative CYE cultures (0.5 ml) at 4×10^8 cfu/ml were fixed for 20 min after transfer to tubes containing 100 μl parafolmadehyde (16%) and 0.2 μl glutaraldehyde (25%). Fixed cells were then immobilized on freshly prepared poly L-lysine-treated slides. Cells were rendered permeable by treatment for 4 min with 1 μg/ml lysozyme treatment. Washing was performed in PBS and probing in PBS 2% BSA with the anti-MreB purified antibodies added at 1:100 dilution. An Alexa-488-coupled anti-rabbit antibody (Molecular Probes) was used as a secondary antibody (1:200). The slides were then mounted in SlowFade Gold anti-fade reagent (Molecular Probes).

Three-dimensional analysis of MreB-stained cells was performed with an inverted Delta Vision optical sectioning microscope (Applied Precision). For high-resolution analysis, we prepared samples directly on a cover slip, instead of a standard immunofluorescence slide, and obtained between 40 and 50 *z* sections spaced at 0.02 μm through the specimen. The images were deconvolved through 15 iterations using the Delta Vision deconvolution software (Applied Precision).

A22 injection experiments and time-lapse fluorescence microscopy

Injection experiments were conducted in a custom diffusion chamber where cells are immobilized on a thin layer of TPM agar and chemicals reach the cells by diffusion through the agar (Ducret *et al*, 2009). Control experiments using fluorescent dyes and metabolic inhibitors showed that chemicals diffuse readily and reversibly to the specimens placed inside the chamber. Injections were performed with a coupled computerized injector system at a 10-μl/s flow rate. Typically, A22 was injected at concentrations ranging between 10 and 150 μg/ml in TPM medium containing glucose 10 mM, which led to reversible, dose-dependent motility arrest. Subsequently, we systematically used 50 μg/ml A22 as it led to motility arrest in >90% of the cells, a dose that did not affect the $mreB_{V323A}$ mutant and was reversed when TPM alone was injected.

For experiments where the A^-S^+ and A^+S^- motile cells were mixed, cells were mixed in a 1:1 ratio. We could discriminate between the strains because the A^-S^+ cells also expressed FrzS–GFP. Experiments using S-motile cells showed that cells in groups were less sensitive to A22: under these conditions complete and reversible block of cell movement was obtained at 150 μg/ml A22. This is presumably because A22 is less accessible to cells within large groups, which was apparent when FrzS–GFP-expressing cells were observed in injection experiments: FrzS–GFP was rapidly dispersed in single cells when A22 was injected at 50 μg/ml, whereas dispersal of FrzS–GFP required a concentration of 150 μg/ml when cells were moving within large S-motile groups (data not shown). Nevertheless, these concentrations remain acceptable because the effect was reversible at 150 μg/ml and this concentration did not affect the $mreB_{V323A}$ mutant.

Images were recorded with a CoolSNAP HQ 2 (Roper Scientific, Roper Scientific SARL, France) and a ×40/0.75 DLL 'Plan-Apochromat' or a ×100/1.4 DLL objective. The resulting images had spatial dimensions of 0.16 and 0.064 μm/pixel, respectively. The excitation beam was emitted by a 120 W metal halide light and signals were monitored using appropriate filters. All fluorescence images were acquired every 2 min (every 30 s for phase acquisition), with a minimal exposure time to minimize bleaching and

phototoxicity effects. As control, a field that was not exposed to fluorescent illumination was monitored under similar conditions. Under the conditions used, the growth or the motility of cells was not affected by the illumination.

Image processing and cell tracking

Subcellular protein localization patterns of wild-type versus *mglA* mutant cells were determined by illuminating the microscopic fields of cells corresponding to each tested strain with similar microscope settings and capturing times. Under these conditions, bipolar FrzS–GFP and AglZ–YFP clusters (polar and internal) were clearly seen in wild-type strains but hardly detectable in the *mglA* mutant. Representative cells of each sub-population were then counted manually. Cell tracking was performed automatically with a home-built macro that runs under the METAMORPH software (Molecular Devices; Ducret *et al*, 2009). When appropriate, manual measurements were also performed to correct tracking errors generated by the software. The data were processed using Excel (Microsoft). Images were processed using ImageJ 1.40g (National Institute of Health, USA) and METAMORPH.

Supplementary data

Supplementary data are available at *The EMBO Journal* Online (http://www.embojournal.org).

Acknowledgements

We acknowledge Felipe Bendezú and Piet de Boer for the generous gift of *E. coli* FB83. We thank Julie Viala, Jennifer Luciano, and all the members of the Zusman and Mignot laboratories for helpful comments and discussion. FM is funded by a thesis fellowship from the Ministère de la Recherche (MENRT). AD is funded by the AFSSET. Research in our laboratories is funded by a grant from the National Institutes of Health to DRZ (GM20509) and by an ANR 'Jeunes Chercheurs-Jeunes Chercheuses' to TM (ANR-07-JCJC-0131).

Conflict of interest

The authors declare that they have no conflict of interest.

References

Arshinoff BI, Suen G, Just EM, Merchant SM, Kibbe WA, Chisholm RL, Welch RD (2007) Xanthusbase: adapting wikipedia principles to a model organism database. *Nucleic Acids Res* **35:** D422–D426

Bean GJ, Flickinger ST, Westler WM, McCully ME, Sept D, Weibel DB, Amann KJ (2009) A22 disrupts the bacterial actin cytoskeleton by directly binding and inducing a low-affinity state in MreB. *Biochemistry* **49:** 4852–4857

Bendezú FO, Hale CA, Bernhardt TG, de Boer PA (2009) RodZ (YfgA) is required for proper assembly of the MreB actin cytoskeleton and cell shape in *E. coli*. *EMBO J* **28:** 193–204

Blackhart BD, Zusman DR (1985) 'Frizzy' genes of *Myxococcus xanthus* are involved in control of frequency of reversal of gliding motility. *Proc Natl Acad Sci USA* **82:** 8767–8770

Bustamante VH, Martinez-Flores I, Vlamakis HC, Zusman DR (2004) Analysis of the Frz signal transduction system of *Myxococcus xanthus* shows the importance of the conserved C-terminal region of the cytoplasmic chemoreceptor FrzCD in sensing signals. *Mol Microbiol* **53:** 1501–1513

Campos JM, Geisselsoder J, Zusman DR (1978) Isolation of bacteriophage MX4, a generalized transducing phage for *Myxococcus xanthus*. *J Mol Biol* **119:** 167–178

Charest PG, Firtel RA (2006) Feedback signaling controls leading-edge formation during chemotaxis. *Curr Opin Genet Dev* **16:** 339–347

Charest PG, Firtel RA (2007) Big roles for small GTPases in the control of directed cell movement. *Biochem J* **401:** 377–390

Defeu Soufo HJ, Graumann PL (2005) *Bacillus subtilis* actin-like protein MreB influences the positioning of the replication machinery and requires membrane proteins MreC/D and other actin-like proteins for proper localization. *BMC Cell Biol* **6:** 10

Divakaruni AV, Baida C, White CL, Gober JW (2007) The cell shape proteins MreB and MreC control cell morphogenesis by positioning cell wall synthetic complexes. *Mol Microbiol* **66:** 174–188

Ducret A, Maisonneuve E, Notareschi P, Grossi A, Mignot T, Dukan S (2009) A microscope automated fluidic system to study bacterial processes in real time. *PLoS One* **4:** e7282

Figge RM, Divakaruni AV, Gober JW (2004) MreB, the cell shape-determining bacterial actin homologue, co-ordinates cell wall morphogenesis in *Caulobacter crescentus*. *Mol Microbiol* **51:** 1321–1332

Gitai Z, Dye N, Shapiro L (2004) An actin-like gene can determine cell polarity in bacteria. *Proc Natl Acad Sci USA* **101:** 8643–8648

Gitai Z, Dye NA, Reisenauer A, Wachi M, Shapiro L (2005) MreB actin-mediated segregation of a specific region of a bacterial chromosome. *Cell* **120:** 329–341

Hartzell P, Kaiser D (1991a) Function of MglA, a 22-kiloDalton protein essential for gliding in *Myxococcus xanthus*. *J Bacteriol* **173:** 7615–7624

Hartzell P, Kaiser D (1991b) Upstream gene of the mgl operon controls the level of MglA protein in *Myxococcus xanthus*. *J Bacteriol* **173:** 7625–7635

Hartzell PL (1997) Complementation of sporulation and motility defects in a prokaryote by a eukaryotic GTPase. *Proc Natl Acad Sci USA* **94:** 9881–9886

Hodgkin J, Kaiser D (1979) Genetics of gliding motility in *Myxococcus xanthus* (Myxobacterales): Two gene systems control movement. *Mol Gen Genet* **171:** 177–191

Iwai N, Nagai K, Wachi M (2002) Novel -benzylisothiourea compound that induces spherical cells in *Escherichia coli* probably by acting on a rod-shape-determining protein(s) other than penicillin-binding protein 2. *Biosci Biotechnol Biochem* **66:** 2658–2662

Jones LJ, Carballido-Lopez R, Errington J (2001) Control of cell shape in bacteria: helical, actin-like filaments in *Bacillus subtilis*. *Cell* **104:** 913–922

Koonin EV, Aravind L (2000) Dynein light chains of the Roadblock/LC7 group belong to an ancient protein superfamily implicated in NTPase regulation. *Curr Biol* **10:** R774–R776

Kortholt A, van Haastert PJ (2008) Highlighting the role of Ras and Rap during *Dictyostelium chemotaxis*. *Cell Signal* **20:** 1415–1422

Kruse T, Moller-Jensen J, Lobner-Olesen A, Gerdes K (2003) Dysfunctional MreB inhibits chromosome segregation in *Escherichia coli*. *EMBO J* **22:** 5283–5292

Leaver M, Errington J (2005) Roles for MreC and MreD proteins in helical growth of the cylindrical cell wall in *Bacillus subtilis*. *Mol Microbiol* **57:** 1196–1209

Leonardy S, Freymark G, Hebener S, Ellehauge E, Sogaard-Andersen L (2007) Coupling of protein localization and cell movements by a dynamically localized response regulator in *Myxococcus xanthus*. *EMBO J* **26:** 4433–4444

Li Y, Sun H, Ma X, Lu A, Lux R, Zusman D, Shi W (2003) Extracellular polysaccharides mediate pilus retraction during social motility of *Myxococcus xanthus*. *Proc Natl Acad Sci USA* **100:** 5443–5448

Mauriello EM, Nan B, Zusman DR (2009) AglZ regulates adventurous (A-) motility in *Myxococcus xanthus* through its interaction with the cytoplasmic receptor, FrzCD. *Mol Microbiol* **72:** 964–977

Mauriello EM, Zusman DR (2007) Polarity of motility systems in *Myxococcus xanthus*. *Curr Opin Microbiol* **10:** 624–629

Mignot T (2007) The elusive engine in *Myxococcus xanthus* gliding motility. *Cell Mol Life Sci* **64:** 2733–2745

Mignot T, Merlie Jr JP, Zusman DR (2005) Regulated pole-to-pole oscillations of a bacterial gliding motility protein. *Science* **310:** 855–857

Mignot T, Shaevitz JW, Hartzell PL, Zusman DR (2007) Evidence that focal adhesion complexes power bacterial gliding motility. *Science* **315:** 853–856

Mohammadi T, Karczmarek A, Crouvoisier M, Bouhss A, Mengin-Lecreulx D, den Blaauwen T (2007) The essential peptidoglycan glycosyltransferase MurG forms a complex with proteins involved in lateral envelope growth as well as with proteins involved in cell division in *Escherichia coli*. *Mol Microbiol* **65:** 1106–1121

Puig O, Caspary F, Rigaut G, Rutz B, Bouveret E, Bragado-Nilsson E, Wilm M, Seraphin B (2001) The tandem affinity purification (TAP) method: a general procedure of protein complex purification. *Methods* **24:** 218–229

Pullman ME, Penefsky HS, Datta A, Racker E (1960) Partial resolution of the enzymes catalyzing oxidative phosphorylation. I. Purification and properties of soluble dinitrophenol-stimulated adenosine triphosphatase. *J Biol Chem* **235:** 3322–3329

Rodriguez AM, Spormann AM (1999) Genetic and molecular analysis of cglB, a gene essential for single-cell gliding in *Myxococcus xanthus*. *J Bacteriol* **181:** 4381–4390

Sliusarenko O, Zusman DR, Oster G (2007) The motors powering A-motility in *Myxococcus xanthus* are distributed along the cell body. *J Bacteriol* **189:** 7920–7921

Slovak PM, Wadhams GH, Armitage JP (2005) Localization of MreB in *Rhodobacter sphaeroides* under conditions causing changes in cell shape and membrane structure. *J Bacteriol* **187:** 54–64

Stephens K, Kaiser D (1987) Genetics of gliding motility in *Myxococcus xanthus*. Molecular cloning of the mgl locus. *Gen Genet* **207:** 256–266

Sun H, Yang Z, Shi W (1999) Effect of cellular filamentation on adventurous and social gliding motility of *Myxococcus xanthus*. *Proc Natl Acad Sci USA* **96:** 15178–15183

Sun H, Zusman DR, Shi W (2000) Type IV pilus of *Myxococcus xanthus* is a motility apparatus controlled by the frz chemosensory system. *Curr Biol* **10:** 1143–1146

Varley AW, Stewart GC (1992) The divIVB region of the *Bacillus subtilis* chromosome encodes homologs of *Escherichia coli* septum placement (minCD) and cell shape (mreBCD) determinants. *J Bacteriol* **174:** 6729–6742

Wall D, Kaiser D (1999) Type IV pili and cell motility. *Mol Microbiol* **32:** 1–10

Ward MJ, Lew H, Zusman DR (2000) Social motility in *Myxococcus xanthus* requires FrzS, a protein with an extensive coiled-coil domain. *Mol Microbiol* **37:** 1357–1371

Wolgemuth C, Hoiczyk E, Kaiser D, Oster G (2002) How myxobacteria glide. *Curr Biol* **12:** 369–377

Wozniak MA, Modzelewska K, Kwong L, Keely PJ (2004) Focal adhesion regulation of cell behavior. *Biochim Biophys Acta* **1692:** 103–119

Yang R, Bartle S, Otto R, Stassinopoulos A, Rogers M, Plamann L, Hartzell P (2004) AglZ is a filament-forming coiled-coil protein required for adventurous gliding motility of *Myxococcus xanthus*. *J Bacteriol* **186:** 6168–6178

Youderian P, Burke N, White DJ, Hartzell PL (2003) Identification of genes required for adventurous gliding motility in *Myxococcus xanthus* with the transposable element mariner. *Mol Microbiol* **49:** 555–570

Yu R, Kaiser D (2007) Gliding motility and polarized slime secretion. *Mol Microbiol* **63:** 454–467

Zusman DR, Scott AE, Yang Z, Kirby JR (2007) Chemosensory pathways, motility and development in *Myxococcus xanthus*. *Nat Rev Microbiol* **5:** 862–872

